dachsous and *frizzled* contribute separately to planar polarity in the *Drosophila* ventral epidermis

Seth Donoughe and Stephen DiNardo*

SUMMARY

Cells that comprise tissues often need to coordinate cytoskeletal events to execute morphogenesis properly. For epithelial tissues, some of that coordination is accomplished by polarization of the cells within the plane of the epithelium. Two groups of genes – the Dachsous (Ds) and Frizzled (Fz) systems – play key roles in the establishment and maintenance of such polarity. There has been great progress in uncovering the how these genes work together to produce planar polarity, yet fundamental questions remain unanswered. Here, we study the *Drosophila* larval ventral epidermis to begin to address several of these questions. We show that *ds* and *fz* contribute independently to polarity and that they do so over spatially distinct domains. Furthermore, we find that the requirement for the Ds system changes as field size increases. Lastly, we find that Ds and its putative receptor Fat (Ft) are enriched in distinct patterns in the epithelium during embryonic development.

INTRODUCTION

Planar polarity refers to the ability of cells to 'know' directional information and to share this information with adjacent cells. Polarity effectors in each cell use that information for many different outputs, including oriented division, directed cell movements and the formation of polarized cell shapes. Together, these outputs enable the many cells that comprise a single tissue to coordinate morphogenic movements.

Genetic experiments in *Drosophila* have been used to identify core planar polarity genes (Vinson and Adler, 1987; Adler et al., 1998). These genes collaborate to produce, amplify and stabilize the initial orienting vector, and thus are required for polarity in many tissues. By their genetic and physical interactions these genes can be grouped into two sets, here called the Frizzled system and the Dachsous system (Axelrod, 2009). It should be noted that, in each system, some of the constituent genes also have roles distinct from their contribution to planar polarity. For example, members of the Dachsous system are important for growth control, whereas members of the Frizzled system participate in canonical Wnt signaling (Kennerdell and Carthew, 1998; Bryant et al., 1988). Our focus here is on the polarity roles of each system.

The Frizzled system comprises the transmembrane proteins Frizzled (Fz), Van Gogh (Vang; also known as Strabismus) and Starry night (Stan; also known as Flamingo), and cytoplasmic proteins such as Dishevelled (Dsh) and Prickle (Pk; also known as Spiny legs). How these proteins interact to generate polarity is not completely clear. It appears that some associations act in a feedback mechanism that can sharpen a subtle, pre-existing bias into a steep intracellular gradient of polarity proteins (Amonlirdviman et al., 2005; Goodrich and Strutt, 2011). Whether this circuit participates in the earlier step of assigning the initial polarity bias is not known. Recent work suggests that polarity might be present much earlier during tissue development than had previously been appreciated (Aigouy et al., 2010), but the source of its initial bias remains elusive.

The Dachsous system is composed of two atypical cadherins, Dachsous (Ds) and Fat (Ft), which are capable of binding one another between neighboring cells. A Golgi-associated kinase, Four-jointed (Fj), promotes the ability of Ft to bind to Ds while inhibiting the ability of Ds to bind to Ft (Simon et al., 2010; Brittle et al., 2010). Thus, a gradient of Ft, Ds or Fj across a tissue could create an asymmetry in Ds-Ft interactions on one cellular interface as compared with the opposite interface. In the wing and eye, there is evidence that the Ds system provides an initial polarizing input, possibly in the form of this asymmetry, which is subsequently sharpened by the Fz system (Yang et al., 2002; Ma et al., 2003). In the adult abdomen, however, the Ds system has been argued to impart polarity independently of the Fz system (Casal et al., 2006).

Although progress has been made to piece together the mechanisms that underlie planar polarity, there are still issues left unresolved. Primary among these is how the Ds and Fz systems each contribute to polarity. It is unclear why they appear to act in sequence in some tissues but not in others. In addition, when the Ds system appears able to directly polarize tissues on its own, it is not known how that signal is converted into polarized outputs. Only a few fly tissues have been used to uncover the interactions between the two polarity systems, and investigating their role in a novel polarized tissue might be revealing.

The *Drosophila* ventral epidermis is one such tissue (Price et al., 2006; Walters et al., 2006; Colosimo and Tolwinski, 2006). In early embryos, the body axis is subdivided into parasegments, each of which is further subdivided into two domains. One half of the epithelial cells will secrete smooth cuticle and the other half will form cuticular protrusions called denticles (the denticle field). The denticle field pattern is the product of a series of distinct polarized events. First, cells align into columns as a consequence of the reorganization of select cell interfaces (Simone and DiNardo, 2010). Second, one to three F-actin bundles protrude from the posterior edge of each cell (Dickinson and Thatcher, 1997; Walters et al., 2006; Price et al., 2006; Colosimo and Tolwinski, 2006). Third, the F-actin bundles guide the secretion of extracellular

University of Pennsylvania Medical School, Department of Cell & Developmental Biology, 421 Curie Blvd, Philadelphia, PA 19104-6048, USA.

*Author for correspondence (sdinardo@mail.med.upenn.edu)

matrix (cuticle) such that denticles take on their final tapered orientation and hooked shapes (Chanut-Delalande et al., 2006; Fernandes et al., 2010; Dilks and DiNardo, 2010). The result is that each column of denticles corresponds to a single column of underlying cells. We take advantage of this polarized pattern to investigate the roles of *ds*, *ft* and *fz* in establishing it.

With each molt, a growing larva secretes a new cuticle that is patterned on the underlying epidermis. Since there are no major cell rearrangements nor any increase in cell number during larval growth, cells of this epithelium maintain their specific fates and relative positions. Thus, the denticle pattern is resynthesized for each successive cuticle, where the columns of protruding denticles remain intact until the next molt, enabling the crawling larvae to grip the substrate during locomotion.

Here we address long-standing questions in the planar cell polarity (PCP) field: (1) how do Fz and the members of the Ds system each contribute to planar polarity in an epithelium and (2) how do Ds and Ft influence the polarized placement of F-actin protrusions?

MATERIALS AND METHODS
Fly stocks
Mutant alleles: *ds[05142]* (FBal0000404), *ds[UAO71]* (FBal0089339), *ft[G-rv]* (FBal0004805), *ft[8]* (FBal0004794), *fj[d1]* (FBal0049500), *fz[15]* (FBal0004931), *fz[21]* (FBal0004937) and *dsh[1]* (FBal0003138). Ectopic Ds signaling was created with *en-Gal4* and *ptc-Gal4* (Bloomington Stock Center) and *UAS-dsΔICD* (a gift from Seth Blair, University of Wisconsin, Madison, WI, USA). Maternal zygotic *ds⁻* animals were created from females with germline *ds[UAO71]* clones – made using *ovo[D1] FRT40A* (FBst0002121) – crossed to *ds[05142] ubi-ECad-GFP/CyO* males, and sorted by the presence of GFP.

Preparation, mounting and microscopy
Larvae were genotyped using the balancers *CyO Act-GFP*, *CyO Kr-Gal4 UAS-GFP* and *TM6b Hu Tb*, rinsed, heated to 65°C (30 minutes) and cleared in Hoyer's solution (Van der Meer, 1977). Cuticles were mounted ventral side up and a coverslip was taped on top, flattening the denticles and preserving their original orientation. Parasegments A4 through A7 were photographed in brightfield using a 40×/0.75 n.a. objective lens.

Fixation and immunofluorescence
Embryos were either heat-fixed (Miller et al., 1989) for rat anti-Ft (1:1600; Ken Irvine, Rutgers University) and rat anti-Ds (1:5000; Michael Simon, Stanford University) stainings or fixed in 4% paraformaldehyde and heptane for 20 minutes and stained with rat anti-Filamin (FBgn0014141) (1:500; Lynn Cooley, Yale University). Mouse anti-phosphotyrosine was used for cell outlines (1:500; Upstate Cell Signaling).

Image analysis
Aside from its role in planar polarization, the Ds system also acts in growth control (Matakatsu and Blair, 2006; Bryant et al., 1988). We found that the Ds system was not essential for growth control in any obvious manner in the ventral epidermis. In *ds* maternal zygotic mutant embryos, for instance, the number of cell columns in the ventral epidermis appeared to be normal. For that reason, henceforth we focus solely on polarity defects.

Cuticles
With anterior to the left, each image was thresholded and then analyzed with the Particles8 plug-in (Gabrial Landini, University of Birmingham, UK). The measurements were exported to a custom Python program that removed out-of-focus and overlapping denticles, leaving ~50% of original denticles. The measurements were used to calculate a single angle for each remaining denticle (see Fig. 1G). Denticles were sorted into bins representing each column. Although columns are somewhat indistinct under some mutant conditions and assignments might be imperfect, our

analysis resulted in clear patterns of column-specific orientation phenotypes, indicating that the technique is nonetheless robust. Presented images were processed in Adobe Photoshop.

Denticle orientations were pooled from each column of each larva and used to calculate the mean vector angle (θ) and length (*r*). Genotypes were then compared on a column-by-column basis following Batschelet's modification for the Mardia-Wheeler-Watson test, as used for two-sample non-parametric analysis of the means of mean angles (Zar, 2010). For Fig. S1 in the supplementary material, we used the homeward component formula (Batschelet, 1981). With images arranged such that the most posteriorly pointing denticles are parallel to the *x*-axis, the resulting formula is: $r\cos(\theta)$. This value ranges from –1.0 for completely anterior to +1.0 for completely posterior.

Rose diagrams were constructed with a custom Python program. The orientations of all denticles from a given column were pooled and presented as a circular frequency plot with 20 isometric bins, each represented by a bar pointing in the direction of the denticles binned therein.

Embryos
To measure actin-based protrusion defects, distances were measured in ImageJ. Cell columns were identified relative to phosphotyrosine enrichments at the 1-2 and 4-5 column interfaces (Simone and DiNardo, 2010).

RESULTS
Two pattern features are apparent on a typical wild-type third instar denticle belt. First, there are seven roughly parallel columns of denticles (numbered 0 through 6; Fig. 1A). This feature exhibits some variability, as the columns are not perfectly aligned (see, for instance, discontinuities along columns 0 and 5 in Fig. 1A), and occasionally there are a few denticles that appear nestled between two columns (note the two denticles between columns 2 and 3 in Fig. 1A; also see Fig. 4A). Second, the denticles within a given column share the same orientation. For instance, denticles of columns 0, 1 and 4 are oriented toward the anterior (left in all images), whereas those of columns 2, 3, 5 and 6 are oriented toward the posterior (right in all images).

Both of these pattern features appeared disordered in *ds⁻* mutants (Fig. 1B). Denticle columns were not as neatly aligned and denticle orientations in most columns were generally more variable. This agrees with the findings presented by Repiso et al. (Repiso et al., 2010), which reported broad denticle field defects in third instar *ds⁻* mutant larvae. To quantitate these defects, we developed a semi-automated method to measure the exact orientation angle of each denticle in a micrograph. This allowed us to score hundreds of individual denticles across many genotypes relatively efficiently, enabling us to examine afresh most of the genotypes presented in Repiso et al. (Repiso et al., 2010), as well as others from several additional experiments.

We used an ImageJ macro to extract denticle orientations and a custom Python program to analyze the results (see Materials and methods for details). Briefly, from each input denticle belt image we measured the angle (Fig. 1G) and relative position of each denticle. Although the denticle columns were not always in perfect register, column placement was consistent enough that the anteroposterior position of a denticle within a belt could be used to assign that denticle to the proper column. A minor drawback was that the extent of the waviness of a column was not directly recorded. This was balanced by the facility to extract orientation data from multiple individuals simultaneously, enabling us to construct a frequency diagram representing the polarity of each column in each genetic background.
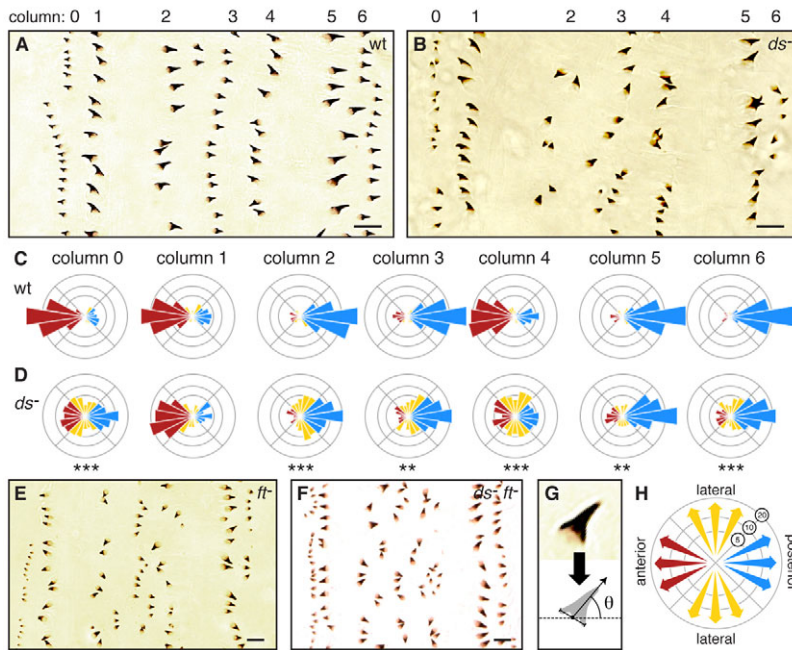
Fig. 1. Ds and Ft are required for denticle field polarity. (**A**,**B**) Wild-type (wt, A) and *ds⁻* (B) third instar *Drosophila* cuticles. Anterior is to the left in this and all subsequent figures. (**C**,**D**) Frequency plots of denticle orientation (see H) in wild-type (*n*=17) and *ds⁻* (*n*=20) cuticles. **P*<0.05, ***P*<0.01, ****P*<0.001, wild type versus *ds⁻* for each denticle column. (**E**,**F**) *ft⁻* and *ds⁻ ft⁻* third instar cuticles. (**G**,**H**) The angle of each denticle (G) displayed as a frequency plot, pooled in color-coded bins (H). Concentric circles represent 5, 10 and 20 percent of all denticles (see text for details). Scale bars: 10 µm.

For the frequency diagrams, orientations were divided into 20 isometric bins, each of which was plotted as an individual bar. Each bar points in the same direction as the denticles that it represents (with anterior to the left and posterior to the right) and the area of the bar corresponds to the percentage of denticles that fall into its range of angles. If a bar extends to the innermost concentric circle, for instance, that bin contains five percent of all denticles scored. Bars are colored for ease of reference based on four quadrants (see Fig. 1H).

Using this representation, wild-type larvae exhibited pronounced column-specific orientation polarity (Fig. 1C). In *ds⁻* larvae, however, polarity was reduced in all columns except for column 1 (Fig. 1D). In some cases, the phenotype was strong: in column 4 of wild type, the vast majority of denticles were oriented anteriorly (red bars), whereas column 4 of *ds⁻* showed approximately equal numbers of denticles oriented in all directions. In other cases, the phenotype was subtler: in column 3 of both wild type and *ds⁻*, there was a tendency to orient toward the posterior (blue bars), yet the breadth of the distribution of orientations was much larger in *ds⁻*, indicating that there was nonetheless a polarity defect.

The degree of disruption is also presented as a single value for each column (see Fig. S1 in the supplementary material). Using such quantification, one can see that in *ds⁻* mutants, polarity was disturbed unevenly across the tissue: columns 0 and 4 were effectively randomized; columns 2, 3, 5 and 6 were rather strongly affected; and column 1 was not affected (see Fig. S1 in the supplementary material). A similar pattern was observed in *ds⁻* maternal zygotic mutants (see Fig. S2E,F in the supplementary material). As noted by Repiso et al. (Repiso et al., 2010), this pattern was also observed in *ft⁻* mutants (Fig. 1E; see Fig. S3E,F in the supplementary material) and *ds⁻ ft⁻* double mutants (Fig. 1F; see Fig. S3G,H in the supplementary material). The fact that the double-mutant phenotype was similar to that of each single mutant is consistent with the current model that Ds and Ft work together to generate planar polarization. The phenotype for *fj⁻* was extremely mild; polarity was detectably different from wild type

only in column 2 (see Fig. S3I,J in the supplementary material). This mild phenotype is not surprising; in other tissues, strong effects are only observed with *fj⁻* mosaics, which cannot be made in this tissue.

Ds extracellular domain can reorient the polarity of neighboring denticle columns

Previous work has shown that abnormally high or low levels of Ds in one cell can reorient the polarity of adjacent cells, presumably by modulating the relative levels of Ds extracellular domain presented to adjacent cells. We sought to determine whether this model was supported in the larval epidermis as well.

A form of Ds with the transmembrane and extracellular domains intact but missing the intracellular domain (*dsΔICD*) was used to create an increased level of Ds signaling emanating from specific cell columns. The polarity of adjacent cell columns was then assessed as described above. We used *en-Gal4* to drive high levels of expression in column 1 and several cell columns anterior to that; *ptc-Gal4* was used to drive high levels of expression in column 2, with lower levels in column 3. The expression domains are represented by purple (*en*) and green (*ptc*) circles around the frequency diagrams in Fig. 2 and Fig. 3. For these experiments, our results were generally in agreement with those described in Repiso et al. (Repiso et al., 2010). In a wild-type background, when *en-Gal4* drove *UAS-dsΔICD* in column 1 (Fig. 2C), the polarity of column 2 was almost completely reversed to point toward the source of the Ds extracellular domain (compare column 2 in Fig. 2B and 2D). Notably, column 3 was also largely reversed, indicating that the repolarizing signal was propagated by column 2 to column 3.

When *ptc-Gal4* was used to drive *UAS-dsΔICD* in column 2 (Fig. 2E), column 3 – where there was also a very low level of ectopic expression – was reoriented to point toward the cell presenting a high level of Ds extracellular domain (Fig. 2F). Column 1 was also partially reversed and there were subtle defects even in columns 0, 4 and 6, possibly indicating that the Ds signal was propagated to the edges of the denticle field.
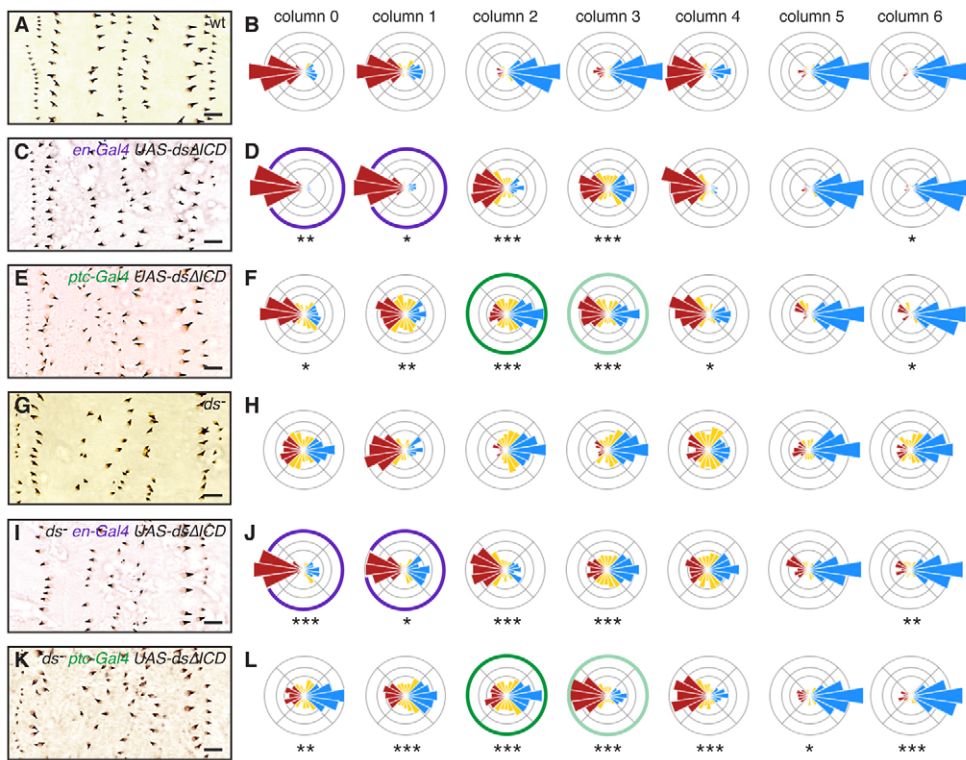
Fig. 2. Ds extracellular domain can reorient neighboring denticle columns. (**A**,**B**) Wild-type (*n*=17), (**C**,**D**) *en-Gal4 UAS-dsΔICD* (*n*=19), (**E**,**F**) *ptc-Gal4 UAS-dsΔICD* (*n*=15), (**G**,**H**) *ds⁻* (*n*=20), (**I**,**J**) *ds⁻ en-Gal4 UAS-dsΔICD* (*n*=29) and (**K**,**L**) *ds⁻ ptc-Gal4 UAS-dsΔICD* (*n*=23) third instar *Drosophila* cuticles. *P<0.05, **P<0.01, ***P<0.001, versus wild type (D,F) or *ds⁻* (J,L). Here and in Fig. 3, colored circles around the frequency diagrams indicate expression of *en-Gal4* (purple) or *ptc-Gal4* (green; intensity indicates level of expression) in those specific columns (Repiso et al., 2010). Scale bars: 10 µm.

These results suggest that the relative levels of Ds extracellular domain on either side of a given column determine its orientation, but such an interpretation might be confounded by the underlying distribution of endogenous Ds across the tissue. Therefore, we conducted the same experiment in a *ds⁻* background, allowing us to isolate the reorientation effect of ectopic Ds signaling from that of background Ds levels. In the *ds⁻* background, *en-Gal4 UAS-dsΔICD* again reoriented column 2 to point toward the source of Ds extracellular domain (Fig. 2I,J), demonstrating that Ds is not required intrinsically for a cell column to receive (and respond to) a Ds signal. In contrast to the effect of such overexpression in the wild-type background, however, column 3 was no longer reoriented

to the same extent (compare Fig. 2D with 2J; *P*<0.001). This demonstrated that Ds is important in propagating the reorienting signal to the next cell column.

When *ptc-Gal4* was used to drive *UAS-dsΔICD* in the *ds⁻* background, the resulting pattern was similar to that in the wild-type background (Fig. 2K,L), but the extent of reorientation in columns 1 and 3 was greater (compare Fig. 2F with 2L; *P*<0.001). We interpreted this result as follows: in the absence of endogenous Ds, columns 1 and 3 were exposed to a higher level of Ds extracellular domain on their interface with column 2 compared with other interfaces; as a consequence, both columns pointed more strongly toward column 2. Column 4 was strongly polarized in *ds⁻ ptc-Gal4*
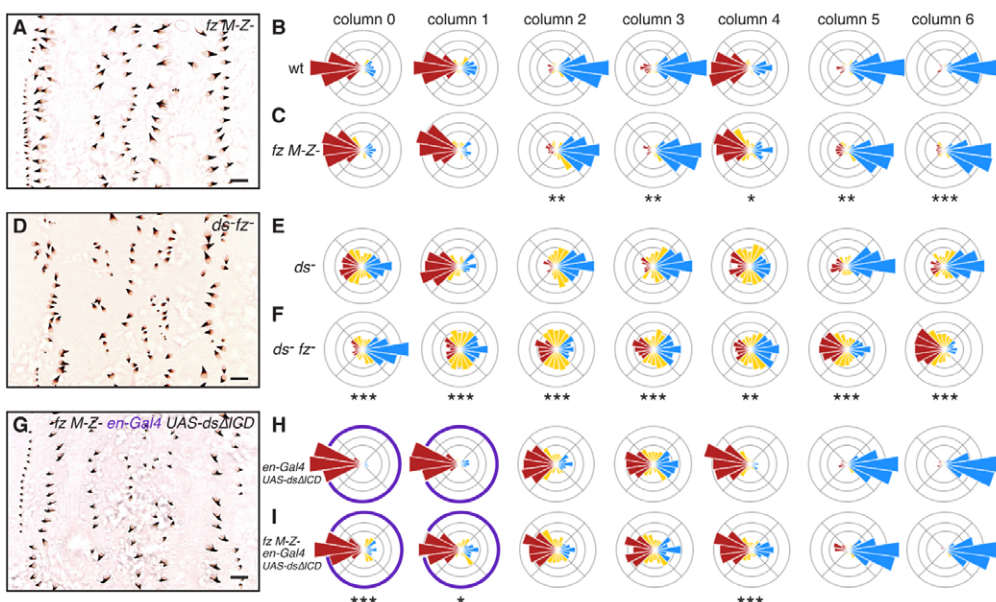

Fig. 3. The role of Fz in denticle field polarity. (**A-C**) Example *fz M⁻Z⁻* cuticle (A) and frequency plot (C; *n*=24), with wild-type plot for comparison (B). (**D-F**) Example *ds⁻ fz⁻* cuticle (D) and frequency plot (F; *n*=22), with *ds⁻* plot for comparison (E). (**G-I**) Example *fz M⁻Z⁻ en-Gal4 UAS-dsΔICD* cuticle (G) and frequency plot (I; *n*=19), with *en-Gal4 UAS-dsΔICD* plot for comparison (H). *P<0.05, **P<0.01, ***P<0.001, between each pair of genotypes. Scale bars: 10 µm.

UAS-dsΔICD, implying that even the low level of ectopic Ds signal presented by column 3 cells was sufficient to reimpose polarity onto the neighboring column. Puzzlingly, columns 0, 5 and 6 were subtly more polarized in *ds⁻ ptc-Gal4 UAS-dsΔICD* compared with *ds⁻*.

Fz has an independent, yet redundant, contribution to polarity in some cell columns

Although the Ds system plays a crucial role in polarizing the denticle field, obvious polarity remains even when Ds is completely absent (see Fig. S2F in the supplementary material). This raised the question of whether the Fz system was responsible for polarizing the denticle field as well.

We could not examine animals that are completely null for several components of the Fz system, such as *stan* or *dsh*, owing to their essential roles in other tissues or signaling pathways. We therefore limited our analysis to larvae that were completely null for Fz protein function or to larvae that carried a PCP-specific mutant allele of *dsh*. In comparison to *ds⁻* or *ft⁻* mutants, *fz⁻* maternal zygotic larvae were found to have a mild phenotype (Fig. 3A) that was not observable by manual scoring alone (Repiso et al., 2010). Denticles in each column were generally oriented in the proper anterior versus posterior direction, but the distribution of orientations from each column was broader (compare Fig. 3B with 3C). For instance, although column 2 denticles in both wild-type and *fz⁻* cuticles were primarily oriented toward the posterior, the distribution of orientations in *fz⁻* was wider. Although subtle, these deviations were statistically significant for columns 2 though 6. Nevertheless, because *fz⁻* mutants exhibited a weaker phenotype than *ds⁻*, Fz cannot be the sole effector of polarity downstream of Ds in this tissue.

Yet, by analyzing *ds⁻ fz⁻* double mutants, it became clear that Fz is nonetheless playing a substantial and redundant role to the Ds system (Fig. 3D). In *ds⁻* cuticles, column 0 was disordered and column 1 pointed anteriorly; in *ds⁻ fz⁻*, column 0 pointed slightly posteriorly and column 1 was completely randomized (compare Fig. 3E with 3F; see Fig. S1 in the supplementary material). The slight polarity remaining in columns 2 and 3 in *ds⁻* was also entirely removed in *ds⁻ fz⁻*. Lastly, in *ds⁻* cuticles, columns 5 and 6 tended to point posteriorly, whereas in *ds⁻ fz⁻* they had a slight tendency to point anteriorly. Taken together, these results signify that (1) the two genes have independent inputs into planar polarity and (2) their relative levels of engagement differ spatially across the tissue.

Although our results suggested that Fz is not essential for Ds-based polarity, it remained possible that Fz plays a subtle role in how a cell responds to a Ds polarity signal. To test whether that was the case, we used *en-Gal4* to overexpress *UAS-dsΔICD* in *fz* null larvae (Fig. 3G). Compared with the effect of such overexpression in a wild-type background, there was a slightly higher level of disorder in columns 0, 1 and 4, which was likely to be due to the slight polarity disruption in *fz⁻* mutants. Importantly, however, the effect on columns 2 and 3 was no different from that of *dsΔICD* overexpression in a wild-type background (compare Fig. 3I with 3H): a high level of Ds extracellular domain presented by column 1 cells was able to reorient cells in columns 2 and 3. Thus, the Ds system is able to send and receive a polarity signal in the complete absence of Fz.

The requirement for Ds changes during larval growth

Over the several days that comprise larval growth, the ventral epidermal cells maintain their relative positions and fates but do not divide. Instead, they increase in ploidy (up to ~64N) and
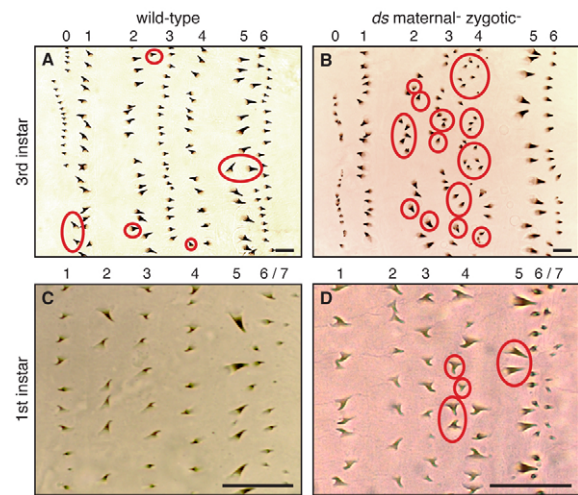

Fig. 4. The requirement for Ds changes during larval growth. (**A**) Wild-type third instar, (**B**) *ds M⁻Z⁻* third instar, (**C**) wild-type first instar and (**D**) *ds M⁻Z⁻* first instar *Drosophila* cuticles. Red ellipses mark 'disrupted' denticles (see text for details). Scale bars: 10 μm.

enlarge dramatically: the width of the denticle field increases by a factor of five. This afforded us the opportunity to test the role played by tissue width in the maintenance of planar polarity by the Ds system. We compared cuticles from first and third instar larvae that were maternally and zygotically null for *ds* (*ds M⁻Z⁻*) this time manually scoring column alignment and denticle orientation. We restricted our analysis to columns 1 through 5, as they are the most regularly constructed in first instar cuticles. A denticle was scored as 'disrupted' (Fig. 4, red ellipses) if it was out of alignment along its presumed column (misplaced) or pointing in the wrong direction (misoriented).

As expected from the analysis above, at third instar, *ds M⁻Z⁻* larvae exhibited many more disruptions than the wild type (compare Fig. 4A with 4B). Given this, it was surprising that in the first instar *ds M-Z-* larvae most denticles appeared to be positioned and oriented normally (compare Fig. 4C with 4D). This shows that, as the ventral epidermis grows, it relies more heavily on Ds to correctly place and orient denticles.

Notably, of the few denticle patterning errors in first instar *ds M⁻Z⁻* larvae, all were misplacements, with no misorientations (see Fig. 4D; see Fig. S4I-L in the supplementary material). This misplacement could have been due to problems in cell alignment (such as extra cells intercalated between cell columns) or to mispositioning of F-actin protrusions within cells (or both), but these possibilities could not be distinguished by examining cuticle patterns alone. To address this, we fixed and stained late stage *ds M⁻Z⁻* embryos to visualize cell outlines and the placement of F-actin protrusions

We did not observe dramatic effects on cell alignment (data not shown), but there were conspicuous defects in F-actin protrusion placement (compare Fig. 5A with 5B; arrows show properly placed protrusions, whereas arrowheads show misplaced protrusions). We analyzed the extent of the defects on a column-by-column basis by measuring where each F-actin protrusion was positioned along the anterior-to-posterior width of each cell (Fig. 5C). Compared with wild type, column 3 was mildly affected, column 4 more strongly affected and column 5 completely disrupted in *ds M⁻Z⁻* embryos (Fig. 5D). This implies that the essential embryonic requirement for Ds is limited to these columns.
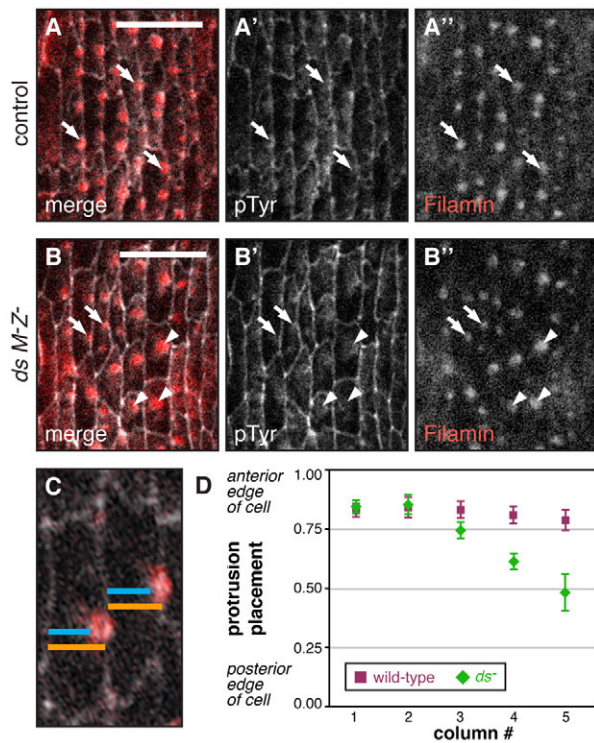
Fig. 5. Actin-based protrusions are misplaced in *ds M⁻Z⁻ Drosophila* embryos. (**A-B″**) Paternal rescue (control, A-A″) and *ds M⁻Z⁻* (B-B″) embryos stained with anti-Filamin and anti-phosphotyrosine (pTyr). Arrows point to posteriorly placed protrusions; arrowheads point to misplaced protrusions. (**C**) Protrusion placement was quantified as the ratio of the distance of a protrusion from the anterior edge of its cell (blue lines) to the anteroposterior width of the cell at that point (orange lines). (**D**) This was plotted for protrusions in cell columns 1-5. Bars indicate 90% confidence interval (*n*=3 embryos each). Despite the slightly misaligned appearance of denticle column cells in *ds⁻* (compare B′ with A′), quantitation has thus far not borne out any consistent, significant difference with wild type. Scale bars: 10 μm.

This finding suggests that the cellular basis of the denticle misplacement phenotype in first instar larval cuticles was the defective placement of F-actin protrusions. It was also interesting that F-actin misplacements in embryos did not necessarily result in misorientations of denticles, at least not during the formation of the first instar cuticle. In the case of wing hairs, the location of actin pre-hair formation along the apical face of a given wing cell is correlated with the eventual orientation of the cuticular hair (Wong and Adler, 1993). Here, by contrast, we did not see evidence for such a correlation. Perhaps in later instars, when cells are much larger, defects in placement of F-actin would lead to misoriented denticles. Alternatively, the lack of a correlation for the first instar cuticle might imply that separate cellular mechanisms are responsible for placing and orienting denticles.

Ds and Ft are enriched in the denticle field

To understand how Ft and Ds polarize the denticle field, it would be informative to know how the proteins are deployed across this tissue. To this end, we stained embryos with anti-Ft and anti-Ds before and during the polarized cell shape changes in the ventral epidermis.

At stage 12, before cell alignment and F-actin protrusion formation, Ft was uniformly localized at cell circumferences, whereas Ds was not easily detected (Fig. 6A,C). By contrast, at stage 13, when cells began to form linear cell columns and just prior to F-actin protrusion formation, both Ft and Ds took on distinct enrichment patterns. Ft was enriched within the denticle field cells, as compared with the smooth field cells. In addition, we observed higher levels centrally within the denticle field, mapping roughly to the 4-5 interface (Fig. 6B′, arrow). By contrast, Ds exhibited a stepped accumulation pattern. It was highly enriched starting at the interface between the column 4 and 5 cells (Fig. 6D′, arrow) and at interfaces posterior to that. It was notably depleted from interfaces that constitute the anterior portion of the denticle field, particularly the 1-2 interface (Fig. 6D′, arrowhead). Within the denticle field cells, neither protein appeared enriched on the long interfaces between the cells of different developing columns, as compared with the interfaces between cells of the same column.

DISCUSSION

We have elucidated the contributions of several key polarity genes in the larval ventral epidermis. The genes in the Ds system are essential for proper polarity in this tissue. Notably, the Ds extracellular domain is able to reorient adjacent cells even when they are null for *ds*. The Fz protein operates largely redundantly and in parallel to the Ds system, and appears to contribute more in some columns than others. As field size increases, it is likely that Fz is less able to polarize the tissue on its own. By contrast, the Ds system is able to polarize the tissue equally well at small and large field sizes. Finally, we find that in embryos, Ds and Ft are enriched in the posterior half of each denticle field. This correlates with the domain of the embryonic denticle field where actin protrusion placement defects appear in *ds M⁻Z⁻* embryos.

The Ds system determines larval epidermal polarity

Several of our observations are in line with what is understood from other tissues. First, the polarity disruptions in *ds⁻* or *ft⁻* single mutants are comparable in severity to those observed in *ds⁻ ft⁻* double mutants. This confirms that Ds and Ft act within the same process to polarize tissues (Matakatsu and Blair, 2004; Casal et al., 2006).

Second, in the adult abdomen, an experimentally induced high point of Ds extracellular domain expression causes an adjacent cell to reorient its polarity toward that high point (Casal et al., 2006). Likewise, overexpression of the Ds extracellular domain in one cell column of an otherwise wild-type larva causes the flanking cell columns to reorient toward this (presumed) enhanced source of Ds (Fig. 2) (Repiso et al., 2010). By repeating this experiment in the *ds⁻* mutant, we avoided any potentially confounding contributions from the superimposed distribution of endogenous Ds. Therefore, we can conclude that cells polarize toward high levels of Ds. Whether this is the case during normal patterning is more difficult to address (see below).

Finally, we found that gain-of-function effects are propagated farther than just the adjacent cell. Thus, in a wild-type background, excess Ds in column 1 caused reorientation in columns 2 and 3 (Fig. 2) (Repiso et al., 2010). This implies that the signal was received in column 2 (resulting in altered polarity there), and then a polarizing effect was propagated to column 3. When such overexpression was repeated in a *ds⁻* background, however, column 2 reoriented whereas column 3 largely did not. This demonstrates
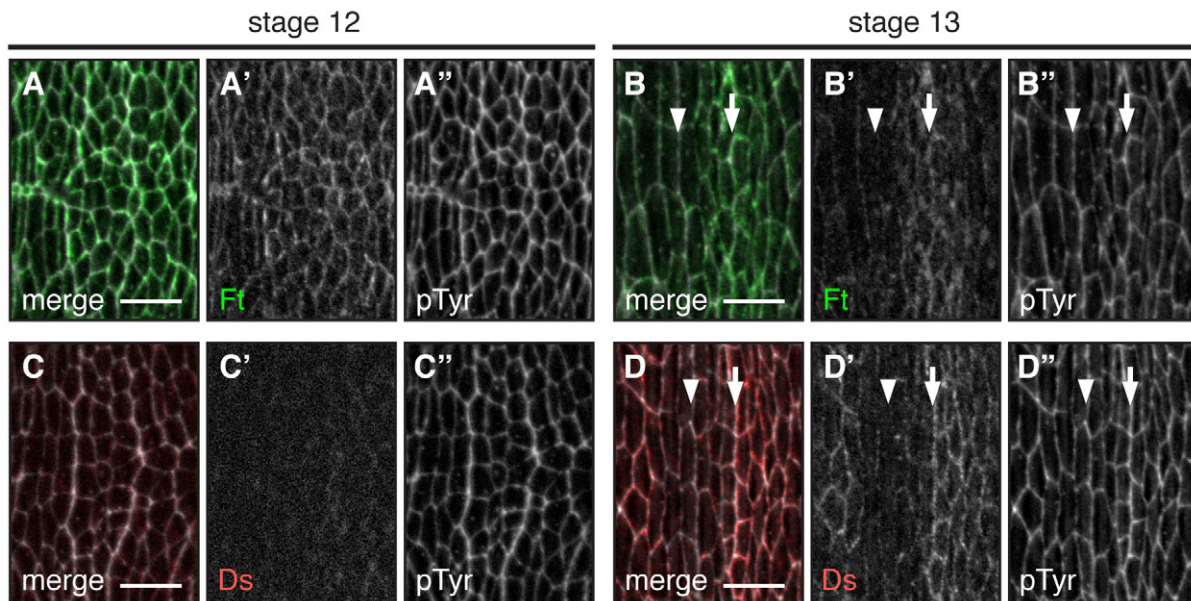
Fig. 6. Ft and Ds localization during epidermal development in *Drosophila*. Stage 12 and 13 embryos stained for (**A-B″**) Ft and pTyr or (**C-D″**) Ds and pTyr. Arrowheads and arrows mark the 1-2 and 4-5 cell column interfaces, respectively. Scale bars: 10 μm.

that Ds is not required for a cell to respond to a Ds polarity signal, but it is important in propagating that signal onward. Altogether, these findings support the hypothesis that Ds and Ft work together to send, implement and propagate a polarity signal.

Ds and Fz have independent inputs to epidermal polarity

A central focus of ongoing research is to determine how the Fz and Ds systems each contribute to the establishment and maintenance of planar polarity. In both the *Drosophila* eye and wing it appears that the Ds system provides a directional cue that is amplified and implemented by the Fz system (Yang et al., 2002; Ma et al., 2003). In the abdomen, by contrast, the Ds system can polarize in the absence of Fz and Stan, both of which are essential for the non-cell-autonomous effects of the Fz system (Casal et al., 2006). Our findings make it clear that for the larval denticle field, the Fz protein acts in a way that is inconsistent with its proposed role downstream of the Ds system. However, this observation still leaves room for the possibility that Ds-Ft engages downstream components within the Fz system (Axelrod, 2009).

We found that the larval epidermis is unique in that the relative requirements for the Ds and Fz systems differ in different domains. The most obvious example of this is that when the Ds system is removed, polarity is completely removed in some columns (e.g. columns 0 and 4) but at least some polarity is still present in others (e.g. columns 1, 2, 3, 5, 6). Thus, it appears that the Fz system (still intact) is acting in those columns to impart polarity, suggesting that the two systems have independent and redundant inputs to polarity.

We also demonstrated that Ds extracellular domain overexpression was able to reorient adjacent columns in an *fz* null background, and this signal was propagated onward. This shows that the Ds system can send, receive and propagate polarity information without contribution from the Fz protein. It remains possible that even when Fz-dependent intercellular signaling is absent, intracellular components of the Fz-system, such as Dsh, act

in implementing the Ds signal (Strutt and Strutt, 2007; Axelrod, 2009). This function of Dsh would have to be unaffected in *dsh[1] MZ* mutants, as the polarity of *dsh[1] MZ* and *dsh[1] MZ ds⁻* larvae appear similar to that of *fz⁻* and *ds⁻ fz⁻* larvae, respectively (see Fig. S3K-N in the supplementary material). Testing for Ds-mediated polarity in *dsh* null cells would be the true test of this hypothesis, but is precluded by the essential role of *dsh* in canonical Wnt signaling.

If, however, the Ds system operates independently of the Fz system, this would have significant ramifications for our understanding of the molecular mechanisms that must be engaged downstream of each polarity system. The two systems must eventually converge at the point when cells create the oriented read-out (in this case, denticle formation). It is possible that the common polarity effectors might be far downstream of the initial effects in signaled cells. Given that the Fz and Ft receptors are so dissimilar from a molecular standpoint, their immediate effectors are likely to be distinct. Only by identifying the proteins that interact with Ft to implement Ds system polarity will we be able to determine whether these effectors intersect downstream components of the Fz system or act independently on the polarity read-out.

Another observation that requires explanation is that the Ds and Fz systems seem to operate serially in some contexts (e.g. in the eye or wing) but in parallel in others (e.g. in the abdomen or the larval epidermis). Ds system-mediated microtubule (MT) orientation has been suggested as one mechanism by which the Ds system could feed into the Fz system (Axelrod, 2009). When MTs are oriented along the axis of polarity of wing cells, MT-mediated polarized transport brings Fz to the cell membrane (Shimada et al., 2006), and it was recently shown that the maintenance of the correct MT orientation is Ds dependent (Harumoto et al., 2010). In the embryonic ventral epidermis, however, MTs are oriented perpendicular to the axis of planar polarity, at least at steady state (Dilks and DiNardo, 2010; Dickinson and Thatcher, 1997). Therefore, unless careful imaging uncovers a minor, posteriorly polarized and Ds-dependent MT track, it seems unlikely that the Ds

system is operating in the ventral epidermis in the manner proposed for wing polarity. This could explain why the Ds system only functions independently of Fz protein in the denticle field.

Residual polarity when both Ds and Fz are removed

In ds^- fz^- larvae, all columns were largely disordered, but the flanking cell columns exhibited a slight, yet statistically significant, tendency toward reversed polarity (see columns 0, 5 and 6 in Fig. 3D; see Fig. S1 in the supplementary material). It is difficult to explain why there is residual polarity rather than randomization. Although the *ds* and *fz* alleles we have used are nulls, we cannot additionally remove *fz2* owing to its essential role in canonical Wnt signaling. Thus, it is possible that Fz2-dependent polarization makes some contribution in the larval epidermis, although Fz2 has not as yet been implicated in PCP in any tissue. Alternatively, even if *fz* were the only Fz system receptor active for PCP, some latent activation of downstream components of the Fz system could, in principle, be responsible for imparting this subtle but polarized output.

An alternative explanation for the residual polarization in ds^- fz^- mutants is that there is an underlying bias in the tissue that is ordinarily masked in the presence of Ds or Fz proteins, but uncovered when both are removed. Since the residual orientation in double mutants tends to be directed away from the smooth field, perhaps that domain is somehow responsible for the latent polarity. Alternatively, the orientation signal might derive from within the denticle field. For instance, the 4-5 column interface is a boundary for Notch and EGFR signaling. Perhaps a low-level orientation signal emanates from that position.

The role of field size in determining polarity strength

Our work also suggests that the Ds and Fz systems have different capacities to adjust to changes in field size. Current models for creating planar polarity begin with a gradient across the field of unpolarized tissue. A subtle bias is presumably then established within each cell across the field, as cells compare the level of the polarizing gradient they detect with that detected by their neighbors. This bias is then reinforced in each cell through a feedback mechanism, converting it into a sharp intracellular gradient of effector protein distribution (Axelrod, 2009). At those initial stages, when a given cell compares the level it perceives with that of adjacent cells, the magnitude of the difference under comparison should be influenced by the size of the field: as field size increases, the contrast perceived by adjacent cells decreases. Correspondingly, any comparison mechanism will be challenged as field size increases.

The larval epidermis presents such a challenge to the polarizing systems as tremendous growth occurs across the field between each larval molt. We were able to analyze the effects on the Fz system as field size increased by examining *ds* null animals at each molt. At small field size (i.e. first instar), polarity defects were rare; however, at large field size (i.e. third instar, five times larger), the disruption to polarity was dramatic (Fig. 4). This suggests that the Fz system loses potency as field size increases. By contrast, the Ds system did not appear to be affected, as there were only rare defects in *fz* null animals at first or third instar (Walters et al., 2006; Price et al., 2006) (Fig. 3A). Since the change in field size through the larval instars occurs in the absence of cell division, it will be of interest to explore what other parameters of cell growth affect the Fz system in this tissue.

Note also that our work demonstrates that denticle field polarity can change over the course of larval growth. This supports the recent finding that third instar polarity is not determined at the embryonic stage (Repiso et al., 2010). Together, these findings strongly imply that planar polarity in the larval epidermis is not permanently set, but rather requires input throughout larval growth.

The cellular basis for denticle polarity

The ventral epidermis also provides the opportunity to study how the two polarity systems influence distinct polarized outputs from the same tissue. Cell alignment and denticle orientation were largely unaffected in ds M^-Z^- embryos/first instar larvae, but there were F-actin protrusion placement defects in cell columns 3 through 5. This result is compelling, as the domain affected matched the region of peak Ds and Ft accumulation. In fz M^-Z^- and $dsh[1]$ MZ backgrounds, there are subtle column 1 and 2 defects in F-actin protrusion placement (Price et al., 2006; Walters et al., 2006). It is intriguing that the embryonic protrusion placement defects appear in complementary patterns for the Fz system as compared with the Ds system; this suggests that in embryos, as in larvae, the two systems function mainly in spatially distinct domains.

Ds and Ft are enriched in the embryonic denticle field

In several tissues, protein distributions have provided a window into the mechanism of polarization (Axelrod, 2001; Strutt, 2001). However, in the embryonic epidermis, our analysis so far has not been suggestive, nor does it support in any simple manner, the model recently proposed by Repiso et al. (Repiso et al., 2010). As neither Ds nor Ft showed an obvious bias toward particular interfaces around a given cell, it is not immediately apparent how these accumulation patterns might be related to proposed Ds-Ft dimer distributions or to the polarity of the tissue. It is of course possible that the protein accumulations would be more suggestive if one could analyze them during the larval molts, but this cannot presently be done.

In this context, it is worth noting that the endogenous distributions of Fz system components have not yet been determined in the ventral epidermis. Staining for Fz-GFP and Dsh-GFP, however, reveals a difference in their enrichments as compared with Ds and Ft: both Fz system members are strongly enriched along cell interfaces that separate cell columns and are depleted from interfaces between cells within the same column (Price et al., 2006). Whether these putative enrichments are necessary for polarity in this tissue remains to be tested.

References
Adler, P. N., Charlton, J. and Liu, J. (1998). Mutations in the cadherin superfamily member gene dachsous cause a tissue polarity phenotype by altering frizzled signaling. *Development* **125**, 959-968.

Aigouy, B., Farhadifar, R., Staple, D. B., Sagner, A., Röper, J.-C., Jülicher, F. and Eaton, S. (2010). Cell flow reorients the axis of planar polarity in the wing epithelium of Drosophila. *Cell* **142**, 773-786.

Amonlirdviman, K., Khare, N. A., Tree, D. R. P., Chen, W.-S., Axelrod, J. D. and Tomlin, C. J. (2005). Mathematical modeling of planar cell polarity to understand domineering nonautonomy. *Science* **307**, 423-426.

Axelrod, J. (2009). Progress and challenges in understanding planar cell polarity signaling. *Semin. Cell Dev. Biol.* **20**, 964-971.

Axelrod, J. D. (2001). Unipolar membrane association of Dishevelled mediates Frizzled planar cell polarity signaling. *Genes Dev.* **15**, 1182-1187.

Batschelet, E. (1981). Measures of dispersion, skewness, and kurtosis. In *Circular Statistics in Biology* (ed. Sibson, R. and Cohen, J. E.), pp. 41-42. New York: Academic Press.

Brittle, A. L., Repiso, A., Casal, J., Lawrence, P. A. and Strutt, D. (2010). Four-jointed modulates growth and planar polarity by reducing the affinity of dachsous for fat. *Curr. Biol.* **20**, 803-810.

Bryant, P. J., Huettner, B., Held, L. I., Ryerse, J. and Szidonya, J. (1988). Mutations at the fat locus interfere with cell proliferation control and epithelial morphogenesis in Drosophila. *Dev. Biol.* **129**, 541-554.

Casal, J., Lawrence, P. A. and Struhl, G. (2006). Two separate molecular systems, Dachsous/Fat and Starry night/Frizzled, act independently to confer planar cell polarity. *Development* **133**, 4561-4572.

Chanut-Delalande, H., Fernandes, I., Roch, F., Payre, F. and Plaza, S. (2006). Shavenbaby couples patterning to epidermal cell shape control. *PLoS Biol.* **4**, e290.

Colosimo, P. F. and Tolwinski, N. S. (2006). Wnt, Hedgehog and junctional Armadillo/beta-catenin establish planar polarity in the Drosophila embryo. *PLoS ONE* **1**, e9.

Dickinson, W. J. and Thatcher, J. W. (1997). Morphogenesis of denticles and hairs in Drosophila embryos: involvement of actin-associated proteins that also affect adult structures. *Cell Motil. Cytoskeleton* **38**, 9-21.

Dilks, S. A. and DiNardo, S. (2010). Non-cell-autonomous control of denticle diversity in the Drosophila embryo. *Development* **137**, 1395-1404.

Fernandes, I., Chanut-Delalande, H., Ferrer, P., Latapie, Y., Waltzer, L., Affolter, M., Payre, F. and Plaza, S. (2010). Zona pellucida domain proteins remodel the apical compartment for localized cell shape changes. *Dev. Cell* **18**, 64-76.

Goodrich, L. V. and Strutt, D. (2011). Principles of planar polarity in animal development. *Development* **138**, 1877-1892.

Harumoto, T., Ito, M., Shimada, Y., Kobayashi, T. J., Ueda, H. R., Lu, B. and Uemura, T. (2010). Atypical cadherins dachsous and fat control dynamics of noncentrosomal microtubules in planar cell polarity. *Dev. Cell* **19**, 389-401.

Kennerdell, J. R. and Carthew, R. W. (1998). Use of dsRNA-mediated genetic interference to demonstrate that frizzled and frizzled 2 act in the wingless pathway. *Cell* **95**, 1017-1026.

Ma, D., Yang, C.-h., McNeill, H., Simon, M. A. and Axelrod, J. D. (2003). Fidelity in planar cell polarity signalling. *Nature* **421**, 543-547.

Matakatsu, H. and Blair, S. S. (2004). Interactions between Fat and Dachsous and the regulation of planar cell polarity in the Drosophila wing. *Development* **131**, 3785-3794.

Matakatsu, H. and Blair, S. S. (2006). Separating the adhesive and signaling functions of the Fat and Dachsous protocadherins. *Development* **133**, 2315-2324.

Miller, K. G., Field, C. M. and Alberts, B. M. (1989). Actin-binding proteins from Drosophila embryos: a complex network of interacting proteins detected by F-actin affinity chromatography. *J. Cell Biol.* **109**, 2963-2975.

Price, M. H., Roberts, D. M., McCartney, B. M., Jezuit, E. and Peifer, M. (2006). Cytoskeletal dynamics and cell signaling during planar polarity establishment in the Drosophila embryonic denticle. *J. Cell Sci.* **119**, 403-415.

Repiso, A., Saavedra, P., Casal, J. and Lawrence, P. A. (2010). Planar cell polarity: the orientation of larval denticles in Drosophila appears to depend on gradients of Dachsous and Fat. *Development* **137**, 3411-3415.

Shimada, Y., Yonemura, S., Ohkura, H., Strutt, D. and Uemura, T. (2006). Polarized transport of Frizzled along the planar microtubule arrays in Drosophila wing epithelium. *Dev. Cell* **10**, 209-222.

Simon, M. A., Xu, A., Ishikawa, H. O. and Irvine, K. D. (2010). Modulation of fat:dachsous binding by the cadherin domain kinase four-jointed. *Curr. Biol.* **20**, 811-817.

Simone, R. P. and DiNardo, S. (2010). Actomyosin contractility and Discs large contribute to junctional conversion in guiding cell alignment within the Drosophila embryonic epithelium. *Development* **137**, 1385-1394.

Strutt, D. I. (2001). Asymmetric localization of frizzled and the establishment of cell polarity in the Drosophila wing. *Mol. Cell* **7**, 367-375.

Strutt, D. and Strutt, H. (2007). Differential activities of the core planar polarity proteins during Drosophila wing patterning. *Dev. Biol.* **302**, 181-194.

Van der Meer, J. M. (1977). Optically clean and permanent whole mount preparation for phase-contrast microscopy of cuticular structures of insect larvae. *Drosoph. Inf. Serv.* **52**, 160.

Vinson, C. R. and Adler, P. N. (1987). Directional non-cell autonomy and the transmission of polarity information by the frizzled gene of Drosophila. *Nature* **329**, 549-551.

Walters, J. W., Dilks, S. A. and Dinardo, S. (2006). Planar polarization of the denticle field in the Drosophila embryo: roles for Myosin II (zipper) and fringe. *Dev. Biol.* **297**, 323-339.

Wong, L. L. and Adler, P. N. (1993). Tissue polarity genes of Drosophila regulate the subcellular location for prehair initiation in pupal wing cells. *J. Cell Biol.* **123**, 209-221.

Yang, C., Axelrod, J. D. and Simon, M. A. (2002). Regulation of Frizzled by fat-like cadherins during planar polarity signaling in the Drosophila compound eye. *Cell* **108**, 675-688.

Zar, J. H. (2010). Circular distributions: hypothesis testing. In *Biostatistical Analysis* (5th edn), pp. 649-650. Upper Saddle River, NJ: Pearson Hall.